AIAA JOURNAL
Vol. 36, No. 11, November 1998

# Structural Damage Identification: A Probabilistic Approach

Loukas Papadopoulos* and Ephrahim Garcia†
*Vanderbilt University, Nashville, Tennessee 37235*

**A method is presented to improve the robustness of current damage detection methodologies. Measured statistical changes in natural frequencies and mode shapes along with a correlated analytical stochastic finite element model are used to assess the integrity of a structure. The approach accounts for variations in the modal properties of a structure (due to experimental errors in the test procedure). A perturbation of the healthy eigenvalue problem is performed to yield the relationship between the changes in eigenvalues and in the global stiffness matrix. This stiffness change is represented as a sum over every structural member by a product of a stiffness reduction factor and a stiffness submatrix. The determination of damaged stiffness statistics permits the comparison of probability density functions between the healthy and estimated damaged stiffnesses. A set of graphical and statistical probability damage quotients are then found that indicate a confidence level on the existence of damage. The effectiveness of the proposed technique is illustrated using simulated data on a three-degree-of-freedom spring–mass system and on an Euler–Bernoulli cantilever aluminum beam.**

## Introduction

THE detection, location, and estimation (DLE) problem of structural damage has been the subject of much current research since the Aloha Boeing 737 accident that occurred on April 28, 1988, which triggered an awareness of the aging of many commercial and military aircraft. In addition, many ground and space structures are often subjected to external hazards. This can come from the hazards of on-orbit existence and or launch loads, for example. Because the expense of maintenance, replacement, and time out of service is costly, it is advantageous to develop methods that can detect, locate, and estimate the extent of damage. The purpose of the current study is to develop a methodology for detecting damage probabilistically using statistically measured experimental modal data from a healthy and damaged structure. A correlated, i.e., model update/refinement has already been performed, analytical stochastic finite element (FE) model, i.e., random mass and stiffness matrices, is also required in the analysis.

Kashangaki[1] provides a concise overview of the on-orbit damage detection and health monitoring process. In addition, Doebling et al.[2] have compiled an extensive review on the subject of damage identification and health monitoring. One approach of the DLE problem adjusts an FE model of the healthy structure to obtain the damaged mass and stiffness matrices based on experimental natural frequencies and mode shapes. Changes in natural frequencies only,[3–5] changes in mode shapes only,[6,7] or both frequency and mode shape changes[8] have been used to indicate the presence of damage. Other researchers use kinetic and strain energies for each mode, such as Chen and Garba[9] and Kashangaki et al.,[10] respectively, to try and estimate the damage. Yet another alternative is a probabilistic approach, which examines the eigenvalue problem from a statistical standpoint by considering eigenvalue and eigenvector uncertainty.[11–15] Although Refs. 11–15 addressed the issue of randomness in structures, their purpose was not to solve the DLE problem. It was not until Ricles and Kosmatka,[16] who utilized mass and stiffness uncertainty to locate potential damaged regions and evaluate the estimate of the damage using the sensitivity analysis of Collins et al.,[15] that the DLE problem was directly addressed. Tavares et al.[17] validated the work of Ricles and Kosmatka[16] using experimentally obtained modal data from a three-dimensional four-bay truss.

A perturbation analysis (similar to that of Cawley and Adams[4] and Hassiotis and Jeong[5]) on the healthy eigenvalue problem is performed to yield the relationship between the changes in eigenvalues and in the global stiffness matrix. The change in global stiffness is expressed as a linear sum of the healthy element stiffness submatrix and a corresponding scaling factor or stiffness reduction factor (SRF).[18] Lim[19] improved the work of White and Maytum[18] and applied the results to the damage detection field.[20] Damage, therefore, will be characterized as a change in stiffness, where these factors indicate the amount of stiffness reduction/increase for each structural element.

A set of simultaneous linear equations that relate the change in eigenvalues to those of the elemental stiffnesses via the SRFs are then obtained. The mean and covariance matrix of the random SRFs that satisfy the described system of algebraic equations need to be calculated. Taking the variance of the described system of algebraic equations results in another set of algebraic equations that relate the covariance matrices of the SRFs and those of the damaged stiffnesses. A Monte Carlo simulation is employed to identify the SRF covariance matrix, which in turn is used to calculate the estimated damaged stiffness covariance matrix. All random distributions, e.g., mass and stiffness matrices, in this work are assumed to be normal. Comparisons of probability density functions between the healthy and damaged stiffnesses yield a set of probability damage quotients (PDQs) that indicate a confidence level on the existence of damage. Therefore, damage will be defined as any value of stiffness not located within the healthy distribution. The effectiveness of the proposed technique is illustrated using simulated data on a three-degree-of-freedom spring–mass system and on an Euler–Bernoulli cantilever beam. The approach is unique in that it accounts for the variability of the structure due to experimental errors in the test procedure.

## Theoretical Development

The free vibration eigenvalue problem for an $N$th-order undamped dynamical system is given by

$$([K] - \lambda_i[M])\{\phi\}_i = \{0\}, \qquad i = 1, 2, 3, \ldots, N \tag{1}$$

where $[M]$ is the $(N \times N)$ symmetric mass matrix, $[K]$ is the $(N \times N)$ symmetric stiffness matrix, $\lambda_i$ is the $i$th mode scalar eigenvalue, and $\{\phi\}_i$ is the $i$th mode eigenvector or mode shape of size $(N \times 1)$. It is tacitly assumed that the eigenvectors are mass normalized, i.e., $\{\phi\}_a^T[M]\{\phi\}_b = \delta_{ab}$, where $\delta_{ab}$ represents the Kronecker delta and is equal to one when $a = b$, otherwise it is equal to zero.

Received Nov. 12, 1996; revision received June 25, 1998; accepted for publication July 5, 1998. 

*Graduate Research Assistant, Center for Intelligent Mechatronics, Department of Mechanical Engineering; currently Senior Mechanical Engineer, Lockheed Martin Missiles and Space Company, Inc., Organization E4-60 Building 104, 1111 Lockheed Martin Way, Sunnyvale, CA 94089-3504. Member AIAA.

†Associate Professor, Center for Intelligent Mechatronics, Department of Mechanical Engineering, Box 1592, Station B. Member AIAA.

Let us assume that Eq. (1) represents the eigenvalue problem of the healthy, predamaged system. The eigenvalue problem of the damaged system can similarly be written as

$$([\tilde{K}] - \tilde{\lambda}_i[\tilde{M}])\{\tilde{\phi}\}_i = \{0\}, \qquad i = 1, 2, 3, \ldots, N \tag{2}$$

where the tilde indicates a damaged quantity. It will be assumed that structural damage affects the stiffness matrix only by an amount $\Delta K$ and that the mass remains constant. Hence, structural damage can be due to cracks or holes affecting the flexural rigidity $EI$. This will produce a change in eigenvalues $\Delta\lambda_i$ and a change in eigenvectors $\{\Delta\phi\}_i$, given by

$$[\tilde{K}] = [K] + [\Delta K] \tag{3}$$

$$[\tilde{M}] = [M] \tag{4}$$

$$\tilde{\lambda}_i = \lambda_i + \Delta\lambda_i \tag{5}$$

$$\{\tilde{\phi}\}_i = \{\phi\}_i + \{\Delta\phi\}_i \tag{6}$$

Substitution of Eqs. (3–6) into Eq. (2) results in, after neglecting multiple products of $\Delta$ quantities (in other words, higher-order terms),

$$\Delta\lambda_i = \frac{\{\phi\}_i^T[\Delta K]\{\phi\}_i}{\{\phi\}_i^T[M]\{\phi\}_i} \tag{7}$$

for $i = 1, 2, 3, \ldots, N$. Equation (7) states that the change in eigenvalues is related to the change in global stiffness through the healthy eigenvectors only and that only the change in eigenvalues is required. This is the expression that Cawley and Adams[4] and Hassiotis and Jeong[5] used in their analyses. If the higher-order terms are kept, the resulting analogous relationship can be written as

$$\Delta\lambda_i = \frac{\{\phi\}_i^T[\Delta K]\{\tilde{\phi}\}_i}{\{\phi\}_i^T[M]\{\tilde{\phi}\}_i} \tag{8}$$

for $i = 1, 2, 3, \ldots, N$. Notice that Eq. (8) has the virtue of using both healthy and damaged eigenvectors. The only major discrepancy between Eqs. (7) and (8) is in the rightmost eigenvector of both numerator and denominator; otherwise, they are identical equations.

The change in global stiffness $[\Delta K]$ is now assumed to be given by the following relationship, as stated by White and Maytum[18]:

$$[\Delta K] = \sum_{j=1}^{L} \alpha_j \left[K_j^e\right] \tag{9}$$

where $L$ is the total number of structural elements, e.g., the total number of aluminum struts in a flexible frame, comprising the system, $\alpha_j$ is the $j$th element SRF, and $[K_j^e]$ is the sparse $j$th element stiffness submatrix (of the same dimension as $[\Delta K]$). The SRFs indicate the amount of stiffness increases/decreases for each $j$th element. A value of $-1$ indicates that there has been a 100% stiffness reduction, and a value of $+1$ indicates a 100% stiffness increase. Substitution of Eq. (9) into Eq. (8) results in

$$\Delta\lambda_i\{\phi\}_i^T[M]\{\tilde{\phi}\}_i = \sum_{j=1}^{L} \alpha_j\{\phi\}_i^T\left[K_j^e\right]\{\tilde{\phi}\}_i \tag{10}$$

for $i = 1, 2, 3, \ldots, N$ from which a set of $N$ simultaneous linear equations with $L$ unknowns can be written in the form

$$[A]_{(N\times L)}\{q\}_{(L\times 1)} = \{b\}_{(N\times 1)} \tag{11}$$

whose elements are given as

$$\begin{aligned} A_{ij} &= \{\phi\}_i^T\left[K_j^e\right]\{\tilde{\phi}\}_i, \qquad q_j = \alpha_j \\ b_i &= \Delta\lambda_i\{\phi\}_i^T[M]\{\tilde{\phi}\}_i = (\tilde{\lambda}_i - \lambda_i)\{\phi\}_i^T[M]\{\tilde{\phi}\}_i \end{aligned} \tag{12}$$

for $i = 1, 2, \ldots, N$, and $j = 1, 2, \ldots, L$. The vector $\{q\}$ in Eq. (11) represents the SRFs for each structural element. In general, the number of experimentally measured modes $N$ will be less than the total number of individual structural elements $L$ of the system. Therefore, the matrix $[A]$ will be rectangular and noninvertible, i.e., Eq. (11) represents a set of underdetermined system of equations. Hassiotis and Jeong[5] handle this case by introducing an optimality criterion into their optimization scheme. For the special case when $N = L$, there will be a unique solution because $[A]$ will be square and invertible. The scenario when $N > L$ (an overdetermined system of equations) will most likely never occur. This paper will focus on the case when $N = L$, thereby permitting a unique solution.

The issue of randomness will now be addressed and the concept of a continuous random variable will be introduced. The probabilistic characteristics of a normal random variable is described by two parameters: the central value and a measure of dispersion or variability, which correspond to a mean $\mu_x$ or expected value $E[x]$ and a variance, from which a normal probability density function (PDF) may be defined as

$$\phi(x) = \frac{1}{\sigma_x\sqrt{2\pi}}\exp\left[-\frac{1}{2}\left(\frac{x-\mu_x}{\sigma_x}\right)^2\right] \tag{13}$$

for $-\infty < x < \infty$. The integral of Eq. (13) is known as a normal cumulative distribution function and is denoted by $\Phi(x)$. Dimensionally, a more convenient measure of dispersion is the square root of the variance, known as the standard deviation $\sigma_x$. Two random variables $x$ and $y$ may also be correlated, which is described by a correlation coefficient or normalized covariance, given by $\rho_{xy} = [\mathrm{cov}(x, y)/\sigma_x\sigma_y]$ with a range of $[-1, +1]$. It is a measure of the degree of (linear) relationship between the variates $x$ and $y$, and a value of zero indicates that the two variables are not correlated. For the present work, all random variables will be assumed to be correlated.

Equation (11), therefore, represents a set of random simultaneous equations, whose properties of $\{q\}$ are to be determined. The SRF distribution will, in general, not be normal, but are assumed to be normal, regardless. The SRF statistical properties are obtained as described by Kleiber and Hien,[21] who state that to a first-order Taylor series approximation the mean value of $\{q\}$ is

$$E([A])_{(N\times L)}E(\{q\})_{(L\times 1)} = E(\{b\})_{(N\times 1)} \tag{14}$$

and the SRF covariance matrix $[S_q]$ is approximately obtained by

$$[S_q]_{(L\times L)} \approx \left[\left.\frac{\partial q}{\partial r}\right|_{r=\bar{r}}\right]_{(L\times P)}[S_r]_{(P\times P)}\left[\left.\frac{\partial q}{\partial r}\right|_{r=\bar{r}}\right]^T_{(P\times L)} \tag{15}$$

where

$$[S_r] = \begin{bmatrix} \mathrm{var}(r_1) & \mathrm{cov}(r_1, r_2) & \cdots & \mathrm{cov}(r_1, r_P) \\ \mathrm{cov}(r_2, r_1) & \mathrm{var}(r_2) & \cdots & \mathrm{cov}(r_2, r_P) \\ \vdots & \vdots & \ddots & \vdots \\ \mathrm{cov}(r_P, r_1) & \mathrm{cov}(r_P, r_2) & \cdots & \mathrm{var}(r_P) \end{bmatrix} \tag{16}$$

$$[S_q] = \begin{bmatrix} \mathrm{var}(\alpha_1) & \mathrm{cov}(\alpha_1, \alpha_2) & \cdots & \mathrm{cov}(\alpha_1, \alpha_L) \\ \mathrm{cov}(\alpha_2, \alpha_1) & \mathrm{var}(\alpha_2) & \cdots & \mathrm{cov}(\alpha_2, \alpha_L) \\ \vdots & \vdots & \ddots & \vdots \\ \mathrm{cov}(\alpha_L, \alpha_1) & \mathrm{cov}(\alpha_L, \alpha_2) & \cdots & \mathrm{var}(\alpha_L) \end{bmatrix} \tag{17}$$

and $[S_r]$ is the covariance matrix of the $P$, i.e., total number of random variables, random structural design parameters (SDPs) and $\bar{r}$ are the corresponding mean values of the random vector $\boldsymbol{r}$. The SDPs consist of healthy and damaged mass and stiffness terms. For example, the SDPs for a two-degree-of-freedom spring-mass system consist of $\{r\} = \{k_1, k_2, m_1, m_2, \tilde{k}_1, \tilde{k}_2, \tilde{m}_1, \tilde{m}_2\}$ (or $\{r\} = \{k_1, k_2, m_1, m_2, \tilde{k}_1, \tilde{k}_2, m_1, m_2\}$ because no mass damage is assumed), where $P = 8$ (four healthy SDPs and four damaged SDPs). The SDP covariance matrix $[S_r]$ is a block diagonal matrix consisting of (for a two-degree-of-freedom spring–mass system)

$$[S_r]_{(8\times 8)} = \begin{bmatrix} [F]_{(4\times 4)} & \vdots & [0]_{(4\times 4)} \\ \cdots & \cdots & \cdots \\ [0]_{(4\times 4)} & \vdots & [\tilde{F}]_{(4\times 4)} \end{bmatrix} \tag{18}$$

$$[F]_{(4\times 4)} = \begin{bmatrix} \mathrm{var}(k_1) & \mathrm{cov}(k_1,k_2) & 0 & 0 \\ \mathrm{cov}(k_1,k_2) & \mathrm{var}(k_2) & 0 & 0 \\ 0 & 0 & \mathrm{var}(m_1) & \mathrm{cov}(m_1,m_2) \\ 0 & 0 & \mathrm{cov}(m_1,m_2) & \mathrm{var}(m_2) \end{bmatrix} \tag{19}$$

$$[\tilde{F}]_{(4\times 4)} = \begin{bmatrix} \mathrm{var}(\tilde{k}_1) & \mathrm{cov}(\tilde{k}_1,\tilde{k}_2) & 0 & 0 \\ \mathrm{cov}(\tilde{k}_1,\tilde{k}_2) & \mathrm{var}(\tilde{k}_2) & 0 & 0 \\ 0 & 0 & \mathrm{var}(m_1) & \mathrm{cov}(m_1,m_2) \\ 0 & 0 & \mathrm{cov}(m_1,m_2) & \mathrm{var}(m_2) \end{bmatrix} \tag{20}$$

and the SRF covariance matrix $[S_q]$ is defined as

$$[S_q]_{(2\times 2)} = \begin{bmatrix} \mathrm{var}(\alpha_1) & \mathrm{cov}(\alpha_1,\alpha_2) \\ \mathrm{cov}(\alpha_1,\alpha_2) & \mathrm{var}(\alpha_2) \end{bmatrix} \tag{21}$$

Similarly, for structures other than spring–mass systems, the mass and stiffness terms given in Eqs. (19) and (20) may correspond to mass $m$ and flexural rigidity $EI$, respectively.

The partial derivatives of $\{q\}$ with respect to the random variables $\boldsymbol{r}$, $\{\partial q/\partial r\}$ in Eq. (15) are given by

$$\left[\frac{\partial q}{\partial r}\right]_{(L\times P)} = \left[\left\{\frac{\partial q}{\partial r_1}\right\}_{(L\times 1)} \quad \left\{\frac{\partial q}{\partial r_2}\right\}_{(L\times 1)} \quad \cdots \quad \left\{\frac{\partial q}{\partial r_P}\right\}_{(L\times 1)}\right] \tag{22}$$

The $\{\partial q/\partial r_u\}$ terms, for $u = 1, 2, \ldots, P$, in Eq. (22) are obtained by differentiating Eq. (11) with respect to $\boldsymbol{r}_u$. Using the product rule of differentiation and rearranging terms slightly results in

$$[A]_{(N\times L)}\left\{\frac{\partial q}{\partial r_u}\right\}_{(L\times 1)} = \left\{\frac{\partial b}{\partial r_u}\right\}_{(N\times 1)} - \left(\left[\frac{\partial A}{\partial r_u}\right]_{(N\times L)}\{q\}_{(L\times 1)}\right) \tag{23}$$

In the general case, $N \neq L$ because the number of unknowns $L$ will greatly exceed the number of measured modes $N$. Therefore, Eq. (14) represents an underdetermined system of equations from which a least-squares technique needs to be employed to solve for $E(\{q\})$. For the ideal case when $N = L$, there will be one unique solution for $E(\{q\})$ because $[A]$ will be square and invertible. The solution of $\{\partial q/\partial r_u\}$ in Eq. (23) will also need to be solved using a least-squares technique, except for the case when $N = L$, where a unique solution exists by inverting $[A]$. The derivatives of $\{b\}$ and $[A]$ with respect to the random variables $\boldsymbol{r}_u$ ($u$th element of vector $\boldsymbol{r}$, which corresponds to a single SDP variable), $\{\partial b/\partial r_u\}$ and $[\partial A/\partial \boldsymbol{r}_u]$, are given in scalar form as, respectively,

$$\frac{\partial b_i}{\partial \boldsymbol{r}_u} = \left(\frac{\partial \tilde{\lambda}_i}{\partial \boldsymbol{r}_u} - \frac{\partial \lambda_i}{\partial \boldsymbol{r}_u}\right)\{\phi\}_i^T[M]\{\tilde{\phi}\}_i + \Delta\lambda_i\left\{\frac{\partial \phi_i}{\partial \boldsymbol{r}_u}\right\}^T[M]\{\tilde{\phi}\}_i + \Delta\lambda_i\{\phi\}_i^T\left[\frac{\partial M}{\partial \boldsymbol{r}_u}\right]\{\tilde{\phi}\}_i + \Delta\lambda_i\{\phi\}_i^T[M]\left\{\frac{\partial \tilde{\phi}_i}{\partial r_u}\right\} \tag{24}$$

$$\frac{\partial A_{ij}}{\partial \boldsymbol{r}_u} = \left\{\frac{\partial \phi_i}{\partial r_u}\right\}^T\left[K_j^e\right]\{\tilde{\phi}\}_i + \{\phi\}_i^T\left[\frac{\partial K_j^e}{\partial \boldsymbol{r}_u}\right]\{\tilde{\phi}\}_i + \{\phi\}_i^T\left[K_j^e\right]\left\{\frac{\partial \tilde{\phi}_i}{\partial r_u}\right\}$$

When $\boldsymbol{r}_u$ represents a healthy SDP, that is, $\{k_1, k_2, \ldots, k_{P/4}, m_1, m_2, \ldots, m_{P/4}\}$, then $\partial\tilde{\lambda}_i/\partial \boldsymbol{r}_u = 0$ and $\{\partial\tilde{\phi}_i/\partial r_u\} = \{0\}$. Similarly, when $r_u$ represents a damaged SDP, that is, $\{\tilde{k}_1, \tilde{k}_2, \ldots, \tilde{k}_{P/4}\}$, $\partial\lambda_i/\partial \boldsymbol{r}_u = 0$, $\{\partial\phi_i/\partial r_u\} = \{0\}$, and $[\partial M/\partial \boldsymbol{r}_u] = [0]$.

The partial derivatives of the healthy and damaged eigenvalues and eigenvectors with respect to the SDPs may be calculated using the work by Fox and Kapoor.[22] For the healthy system, eigenvalues and eigenvectors are stated as

$$\frac{\partial \lambda_i}{\partial \boldsymbol{r}_u} = \{\phi\}_i^T\left[\frac{\partial [K]}{\partial \boldsymbol{r}_u} - \lambda_i\frac{\partial [M]}{\partial \boldsymbol{r}_u}\right]\{\phi\}_i \tag{25}$$

$$\frac{\partial \{\phi\}_i}{\partial \boldsymbol{r}_u} = -\left([F_i][F_i] + 2[M]\{\phi\}_i\{\phi\}_i^T[M]\right)^{-1} \times \left([F_i]\left[\frac{\partial F_i}{\partial \boldsymbol{r}_u}\right] + [M]\{\phi\}_i\{\phi\}_i^T\frac{\partial [M]}{\partial \boldsymbol{r}_u}\right)\{\phi\}_i \tag{26}$$

where

$$[F_i] = ([K] - \lambda_i[M])$$
$$\left[\frac{\partial F_i}{\partial \boldsymbol{r}_u}\right] = \left(\frac{\partial [K]}{\partial \boldsymbol{r}_u} - \lambda_i\frac{\partial [M]}{\partial \boldsymbol{r}_u} - \frac{\partial \lambda_i}{\partial \boldsymbol{r}_u}[M]\right) \tag{27}$$

To obtain the damaged eigenderivatives, Eqs. (25–27) may also be used by replacing the healthy parameters with their corresponding damaged counterparts or tilde quantities. The only requirement in Eqs. (25–27) is that the eigenvectors $\{\phi\}_i$ be mass normalized. Hasselman and Hart[12] state that the mean values for the eigenvalues and eigenvectors are obtained from an eigenvalue analysis where the mass and stiffness matrices are formed using the mean SDPs, i.e., $\bar{r}$.

Equation (14) stipulates that the mean SRFs are solved by using the mean values for $[A]$ and $\{b\}$. It turns out, however, that the SRF covariance matrix $[S_q]$ will not be calculated using Eq. (15), but instead will be calculated using a Monte Carlo analysis performed on Eq. (11). The reason for this is that Eq. (15) has unknowns on both sides of the equal sign. The SRF covariance matrix is certainly an unknown, and although the healthy SDP terms in Eq. (19) are known, the damaged ones, i.e., upper left quadrant of $[\tilde{F}]$, in Eq. (20) are not. Values of $[A]$ and $\{b\}$ are generated at random according to Eq. (12), and Eq. (11) is used to solve for the SRFs. After many consecutive Monte Carlo runs, the stored SRF values are used to compute the SRF covariance matrix.

Once the statistics of the SRFs are computed from the Monte Carlo simulation, the statistics of the estimated damaged stiffnesses can be computed. Substitution of Eq. (9) into Eq. (3) results in

$$[\tilde{K}] = \sum_{j=1}^{L}\left[\tilde{K}_j^e\right] = \sum_{j=1}^{L}(1+\alpha_j)\left[K_j^e\right] \tag{28}$$

where an elemental matrix expression for the $j$th damaged stiffness is written as

$$\left[\tilde{K}_j^e\right] = (1+\alpha_j)\left[K_j^e\right] \tag{29}$$

In general, there is a common factor in all of the matrix elements of Eq. (29), such as the flexural rigidity $EI$ for an Euler–Bernoulli beam (excluding axial deformation). This common factor can effectively be pulled out of each matrix (the remaining terms in the matrix are just connectivity information of the structure, which are no longer required) and a scalar version of Eq. (29) is written as

$$\tilde{k}_j = (1+\alpha_j)k_j = k_j + \alpha_j k_j \tag{30}$$

The exact mean properties of $\tilde{k}_j$ are computed by taking the expected value of Eq. (30), given by

$$E(\tilde{k}_j) = E(k_j + \alpha_j k_j) = E(k_j) + E(\alpha_j k_j) \tag{31}$$

The rightmost term on the right-hand side of Eq. (31) represents the joint second moment of $\alpha_j$ and $k_j$ and is defined as

$$E(\alpha_j k_j) = \mathrm{cov}(\alpha_j, k_j) + E(\alpha_j)E(k_j) \tag{32}$$

Substitution of Eq. (32) into Eq. (31) and combination of terms yield

$$E(\tilde{k}_j) = [1 + E(\alpha_j)]E(k_j) + \mathrm{cov}(\alpha_j, k_j) \tag{33}$$

Because $\alpha_j$ and $k_j$ are uncorrelated random variables, i.e., $\mathrm{cov}(\alpha_j, k_j) = 0$ because the value of the SRF should not depend in any way on the value of the healthy stiffness, Eq. (33) simplifies to

$$E(\tilde{k}_j) = [1 + E(\alpha_j)]E(k_j) \tag{34}$$

The covariance matrix for the estimated damaged stiffnesses is computed (shown here for a one-dimensional two-degree-of-freedom spring–mass system) by substituting Eqs. (18–22) into Eq. (15) and

carrying out the matrix multiplications. The resulting expressions are written in matrix form as

$$[A^*]_{(3\times 3)}\{q^*\}_{(3\times 1)} = \{b^*\}_{(3\times 1)} \tag{35}$$

where

$$[A^*] = \begin{bmatrix} \left(\frac{\partial q_1}{\partial \tilde{k}_1}\right)^2 & 2\left(\frac{\partial q_1}{\partial \tilde{k}_1}\right)\left(\frac{\partial q_1}{\partial \tilde{k}_2}\right) & \left(\frac{\partial q_1}{\partial \tilde{k}_2}\right)^2 \\ \left(\frac{\partial q_1}{\partial \tilde{k}_1}\right)\left(\frac{\partial q_2}{\partial \tilde{k}_1}\right) & \left[\left(\frac{\partial q_1}{\partial \tilde{k}_1}\right)\left(\frac{\partial q_2}{\partial \tilde{k}_2}\right) + \left(\frac{\partial q_1}{\partial \tilde{k}_2}\right)\left(\frac{\partial q_2}{\partial \tilde{k}_1}\right)\right] & \left(\frac{\partial q_1}{\partial \tilde{k}_2}\right)\left(\frac{\partial q_2}{\partial \tilde{k}_2}\right) \\ \left(\frac{\partial q_2}{\partial \tilde{k}_1}\right)^2 & 2\left(\frac{\partial q_2}{\partial \tilde{k}_1}\right)\left(\frac{\partial q_2}{\partial \tilde{k}_2}\right) & \left(\frac{\partial q_2}{\partial \tilde{k}_2}\right)^2 \end{bmatrix} \tag{36}$$

$$\{q^*\} = \begin{Bmatrix} \mathrm{var}(\tilde{k}_1) \\ \mathrm{cov}(\tilde{k}_1, \tilde{k}_2) \\ \mathrm{var}(\tilde{k}_2) \end{Bmatrix} \tag{37}$$

$$\{b^*\} = \begin{Bmatrix} \mathrm{var}(\alpha_1) - d_1 - d_2 \\ \mathrm{cov}(\alpha_1, \alpha_2) - d_3 - d_4 \\ \mathrm{var}(\alpha_2) - d_5 - d_6 \end{Bmatrix} \tag{38}$$

$$\begin{Bmatrix} d_1 \\ d_2 \\ d_3 \\ d_4 \\ d_5 \\ d_6 \end{Bmatrix} = \begin{Bmatrix} f\left(\frac{\partial q_1}{\partial k_1}\right)^2 + 2g\left(\frac{\partial q_1}{\partial k_1}\right)\left(\frac{\partial q_1}{\partial k_2}\right) + h\left(\frac{\partial q_1}{\partial k_2}\right)^2 \\ 2i\left(\frac{\partial q_1}{\partial m_1}\right)^2 + 4j\left(\frac{\partial q_1}{\partial m_1}\right)\left(\frac{\partial q_1}{\partial m_2}\right) + 2k\left(\frac{\partial q_1}{\partial m_2}\right)^2 \\ f\left(\frac{\partial q_1}{\partial k_1}\right)\left(\frac{\partial q_2}{\partial k_1}\right) + g\left[\left(\frac{\partial q_1}{\partial k_1}\right)\left(\frac{\partial q_2}{\partial k_2}\right) + \left(\frac{\partial q_1}{\partial k_2}\right)\left(\frac{\partial q_2}{\partial k_1}\right)\right] + h\left(\frac{\partial q_1}{\partial k_2}\right)\left(\frac{\partial q_2}{\partial k_2}\right) \\ 2i\left(\frac{\partial q_1}{\partial m_1}\right)\left(\frac{\partial q_2}{\partial m_1}\right) + 2j\left[\left(\frac{\partial q_1}{\partial m_1}\right)\left(\frac{\partial q_2}{\partial m_2}\right) + \left(\frac{\partial q_1}{\partial m_2}\right)\left(\frac{\partial q_2}{\partial m_1}\right)\right] + 2k\left(\frac{\partial q_1}{\partial m_2}\right)\left(\frac{\partial q_2}{\partial m_2}\right) \\ f\left(\frac{\partial q_2}{\partial k_1}\right)^2 + 2g\left(\frac{\partial q_2}{\partial k_1}\right)\left(\frac{\partial q_2}{\partial k_2}\right) + h\left(\frac{\partial q_2}{\partial k_2}\right)^2 \\ 2i\left(\frac{\partial q_2}{\partial m_1}\right)^2 + 4j\left(\frac{\partial q_2}{\partial m_1}\right)\left(\frac{\partial q_2}{\partial m_2}\right) + 2k\left(\frac{\partial q_2}{\partial m_2}\right)^2 \end{Bmatrix}_{(6\times 1)} \tag{39}$$

and $f = \mathrm{var}(k_1)$, $g = \mathrm{cov}(k_1, k_2)$, $h = \mathrm{var}(k_2)$, $i = \mathrm{var}(m_1)$, $j = \mathrm{cov}(m_1, m_2)$, and $k = \mathrm{var}(m_2)$.

Once the statistical properties of the estimated damaged stiffnesses are determined by Eqs. (34) and (35), they are probabilistically compared to the healthy stiffnesses to yield an estimate of the probability of damage. The two techniques employed to determine the probability of damage are the graphical and statistical approaches. The graphical approach is accomplished by comparing the two PDFs, as described by Eq. (13), for both healthy and damaged systems. Consider two normal PDF distributions, $\phi_1(x)$ and $\phi_2(x)$, with parameters $(\mu_1, \sigma_1)$ and $(\mu_2, \sigma_2)$, respectively. Equating $\phi_1(x)$ and $\phi_2(x)$ and combining terms result in the following quadratic equation:

$$\hat{a}x^2 + \hat{b}x + \hat{c} = 0 \tag{40}$$

where $\hat{a} = (\sigma_2^2 - \sigma_1^2)$, $\hat{b} = 2(\mu_2\sigma_1^2 - \mu_1\sigma_2^2)$, and $\hat{c} = \mu_1^2\sigma_2^2 - \mu_2^2\sigma_1^2 - 2\sigma_1^2\sigma_2^2\,\ln(\sigma_2/\sigma_1)$, whose roots $x$ and $y$ are given by

$$\hat{q} = -\tfrac{1}{2}\left\{\hat{b} + \mathrm{sgn}(\hat{b})\ \sqrt{\hat{b}^2 - 4\hat{a}\hat{c}}\right\}$$
$$x = \hat{q}/\hat{a}, \qquad y = \hat{c}/\hat{q} \tag{41}$$

and $x_1 = \mathrm{minimum}(x, y)$ and $x_2 = \mathrm{maximum}(x, y)$.

The two PDF curves will then have exactly two intersection points, which are used to calculate the area of intersection. The area of intersection is composed of three sections and is given by Eq. (42). The first area is evaluated from an $x$ range of $[-\infty, x_1]$, the second from $[x_1, x_2]$, and the third from $[x_2, +\infty]$ using either the healthy or damaged PDF statistics for $(\mu_a, \sigma_a)$, $(\mu_b, \sigma_b)$, and $(\mu_c, \sigma_c)$:

$$\begin{aligned} \mathrm{area}_1 &= \Phi\left(\frac{x_1 - \mu_a}{\sigma_a}\right) - \Phi\left(\frac{-\infty - \mu_a}{\sigma_a}\right) = \Phi\left(\frac{x_1 - \mu_a}{\sigma_a}\right) \\ \mathrm{area}_2 &= \Phi\left(\frac{x_2 - \mu_b}{\sigma_b}\right) - \Phi\left(\frac{x_1 - \mu_b}{\sigma_b}\right) \\ \mathrm{area}_3 &= \Phi\left(\frac{+\infty - \mu_c}{\sigma_c}\right) - \Phi\left(\frac{x_2 - \mu_c}{\sigma_c}\right) = 1 - \Phi\left(\frac{x_2 - \mu_c}{\sigma_c}\right) \end{aligned} \tag{42}$$

The parameters $(\mu_a, \sigma_a)$, $(\mu_b, \sigma_b)$, and $(\mu_c, \sigma_c)$ come from the distributions of either $\phi_1(x)$ or $\phi_2(x)$ depending on satisfaction of the following criteria: minimum$[\phi_1(0.99x_1), \phi_2(0.99x_1)]$, minimum$[\phi_1(x_2 - 0.01\Delta x), \phi_2(x_2 - 0.01\Delta x)]$, $\Delta x = x_2 - x_1$, and minimum$[\phi_1(1.01x_2), \phi_2(1.01x_2)]$, respectively. This can best be illustrated by considering the following two distributions: $(\mu_1, \sigma_1) = (7.5, 1.0)$ and $(\mu_2, \sigma_2) = (8.0, 0.5)$. Applying Eqs. (40) and (41) results in $\hat{a} = -0.75$, $\hat{b} = 12.25$, and $\hat{c} = -49.59$ with roots $x_1 = 7.41$ and $x_2 = 8.92$. The three PDF areas of intersection area$_1$ (lightly shaded region), area$_2$ (vertically hatched, medium shaded region), and area$_3$ (darkly shaded region), whose ranges are $[-\infty, 7.41]$, $[7.41, 8.92]$, and $[8.92, +\infty]$, respectively, are shown in Fig. 1. The parameters of $(\mu_a, \sigma_a)$ come from the second distribution

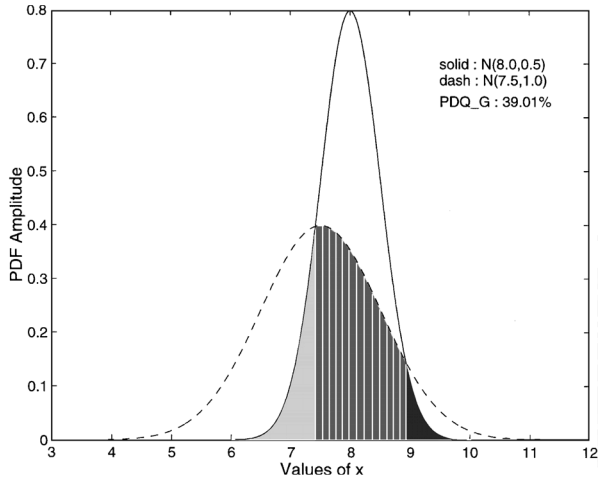


**Fig. 1 PDF comparison of two distributions showing all three areas of intersection using the graphical approach.**

$(\mu_2, \sigma_2)$ because minimum$[\phi_1(7.34), \phi_2(7.34)]$ = minimum$[0.394, 0.334] = 0.334$. Similarly, the parameters of $(\mu_b, \sigma_b)$ come from the first distribution $(\mu_1, \sigma_1)$ because minimum$[\phi_1(8.90), \phi_2(8.90)]$ = minimum$[0.15, 0.158] = 0.15$. Finally, the parameters of $(\mu_c, \sigma_c)$ come from the second distribution $(\mu_2, \sigma_2)$ because minimum$[\phi_1(9.01), \phi_2(9.01)]$ = minimum$[0.128, 0.104] = 0.104$. Using Eq. (42), $\text{area}_1$ represents 11.88% of the total area, $\text{area}_2$ 45.88%, and $\text{area}_3$ 3.23%, for a total of area of 60.99%.

This area of intersection or graphical probability health quotient gives a probability estimate of how closely the two curves are related from a graphical viewpoint. The greater the shared area, the more related the curves become. Because the graphical area of intersection gives an indication of how related the two PDF curves are, then the graphical probability damage quotient (PDQ-G), defined as

$$\text{PDQ-G} = 1 - (\text{area}_1 + \text{area}_2 + \text{area}_3) \tag{43}$$

gives an indication of how unrelated they are. The PDQ-Gs have a range of $[0, +1]$, where a value of zero indicates that the two PDF curves are exactly the same, hence no damage, and a value of one indicates that the stiffness values from the healthy and damaged curves are not related in any way, indicating that damage has occurred. Every element of the structure would be analyzed in this manner and given a PDQ-G in accordance with Eq. (43). Applying Eq. (43) to the example yields a value of PDQ-G = 0.3901. This indicates that there is a 39.01% probability that the two distributions are different.

The statistical approach is based on computing the amount of damaged stiffness PDF area contained within a defined healthy interval. A range of healthy stiffnesses defines the interval limits from which the damaged stiffness PDF curve is evaluated. Mathematically, the statistical probability health quotient (PHQ-S) is defined as

$$\text{PHQ-S} = P(a_i < \tilde{K}_i \le b_i) = \int_{a_i}^{b_i} \phi_{\tilde{K}_i}(\tilde{k}_i)\, \mathrm{d}\tilde{k}_i \tag{44}$$

where $a_i = \mu_{k_i} - n\sigma_{k_i}$ and $b_i = \mu_{k_i} + n\sigma_{k_i}$ define the lower and upper limits, respectively, of the healthy stiffness interval for structural element $i$. $N(\mu_{k_i}, \sigma_{k_i})$ defines the healthy stiffness distribution for element $i$, and $N(\mu_{\tilde{k}_i}, \sigma_{\tilde{k}_i})$ defines the $i$th damaged stiffness distribution. The value of $n$ denotes the number of healthy stiffness standard deviations away from the mean value (used to define the healthy interval). Note that $a \pm 1\sigma$ interval $(n = 1)$ encompasses 68.3% of the total area. Similarly, $a \pm 2\sigma$ interval $(n = 2)$ encompasses 95.4% and $a \pm 3\sigma$ interval $(n = 3)$ encompasses 99.7%. The choice for $n$ is subjective and depends on the believability of the healthy PDF stiffnesses.

The PHQ-S yields the probability that the stiffnesses from the damaged distribution are shared by the healthy distribution.

**Table 1 Comparison of PDQ-S for a $\pm 1\sigma$, $\pm 2\sigma$, and $\pm 3\sigma$ healthy interval, as well as the PDQ-G value**

| $\pm n\sigma$ Interval | PDQ-S, % | PDQ-G, % |
|---|---|---|
| 1 | 65.87 | N/A |
| 2 | 37.53 | 39.01 |
| 3 | 18.14 | N/A |

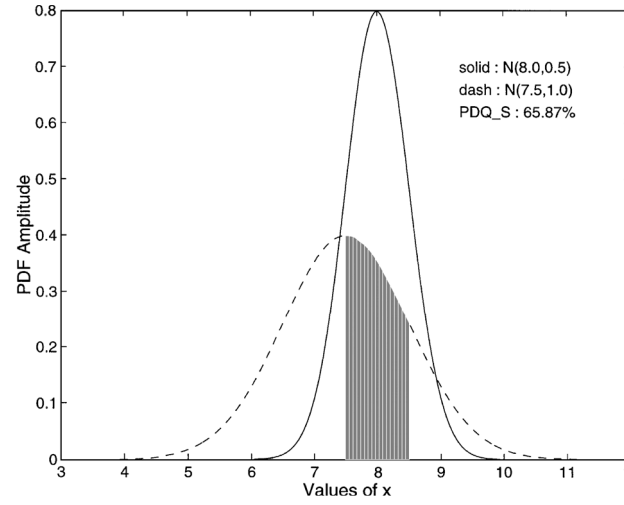


**Fig. 2 PDF comparison of two distributions using the statistical approach for a $\pm 1\sigma$ healthy interval.**

Consequently, the statistical probability damage quotient (PDQ-S) is written as

$$\text{PDQ-S} = 1 - \text{PHQ-S} = 1 - \left[\Phi_{\tilde{K}_i}\left(\frac{b_i - \mu_{\tilde{k}_i}}{\sigma_{\tilde{k}_i}}\right) - \Phi_{\tilde{K}_i}\left(\frac{a_i - \mu_{\tilde{k}_i}}{\sigma_{\tilde{k}_i}}\right)\right] \tag{45}$$

Damage will, therefore, be defined as any value of stiffness not located within the healthy interval, and the PDQ-S gives the probability of the occurrence of this event for each structural member of the system. Consider the example with the two normal distributions: $(\mu_1, \sigma_1) = (7.5, 1.0)$ and $(\mu_2, \sigma_2) = (8.0, 0.5)$. Table 1 lists the PDQ-S using $\pm 1\sigma$, $\pm 2\sigma$, and $\pm 3\sigma$ healthy intervals. Figure 2 shows graphically the healthy area underneath the damaged PDF curve for a $\pm 1\sigma$ interval. Table 1 indicates that as the healthy interval increases, the PDQ-S decreases (which is expected). Notice also that the PDQ-S at the $\pm 2\sigma$ interval (37.53%) is approximately the same as the PDQ-G (39.01%). It should be pointed out, however, that neither PDQ-G (or PDQ-S) nor the SRF statistics alone should solely be employed to make a statement about the damage; rather, they should be used in tandem.

The overall process of probabilistically solving the DLE problem is stated in the following 10 steps:

1) Determine the statistical properties of the healthy mass and stiffness parameters of the system. It is tacitly assumed that the healthy FE model correctly describes the statistics of the healthy experimental modal data, i.e., model update/refinement has been performed.

2) Determine the mean healthy natural frequencies and mode shapes of the system (whether from the healthy experiment or from the updated FE model).

3) Determine the mean damaged natural frequencies and mode shapes of the system from the experiment.

4) From Eq. (14) solve for the mean SRFs.

5) Using step 4, the mean estimated damaged stiffness matrix is calculated using Eq. (28), as well as the mean estimated damaged elemental stiffness values using Eq. (34).

6) Using the eigenvalue and eigenvector derivatives, Eqs. (25–27), $\{\partial q/\partial r\}$ from Eq. (22) is obtained in conjunction with Eqs. (23) and (24).

7) A Monte Carlo simulation performed on Eq. (11) determines the SRF covariance matrix $[S_q]$. As a check, the mean SRFs from the Monte Carlo simulation are compared to those of step 4.

8) Using Eqs. (35–39), the covariance matrix of the estimated damaged stiffnesses is calculated. The estimated damaged stiffness standard deviations are then determined.

9) The PDF intersection properties are then computed by Eqs. (40) and (41) using the statistics of the estimated damaged stiffnesses (steps 5 and 8) and the statistics of the healthy stiffnesses (step 1).

10) PDQs are assigned to each structural member in accordance with the graphical form, Eq. (43), or the statistical form, Eq. (45).

A final note should be made concerning step 1. Although this paper addresses the damage DLE problem, the same procedure can also be used to probabilistically solve the model update/refinement problem. For this scenario, the SRFs do not indicate potential damage locations; rather, they indicate locations required to be modified to adjust the initial stochastic FE model to correctly match the statistics of the healthy experimental modal data. Likewise, the healthy natural frequencies $\lambda_i$ and mode shapes $\{\phi_i\}$ would correspond to an eigenanalysis of the initial FE model. The damaged natural frequencies $\tilde{\lambda}_i$ and mode shapes $\{\tilde{\phi}_i\}$ would correspond to the healthy experimental modal data.

## Results

To illustrate the proposed method, the theory will be applied to the identification of damage in a one-dimensional three-degree-of-freedom spring–mass system and in an Euler–Bernoulli cantilever beam. Both examples deal with simulated data and assume that the healthy FE models of both systems accurately describe the system before damage; hence, no model updating will be required. The SDP parameters are assumed to be correlated normal random variables with arbitrarily selected values for both the healthy and damaged distributions. It is also assumed that the eigenanalyses from these arbitrarily chosen distributions agree with the modal parameters obtained from experiment (if an experiment was conducted). A short notation that will be used to describe the parameters of a normal distribution is $N(\mu, \sigma)$. Assume that all SDP values are of SI units, e.g., mass in kilograms and stiffness in Newton per meter. Damage will take the form of a change in stiffness only, and mass is assumed unchanged. The method was applied to an ideal condition where $N = L$; therefore, $[A]$ in Eq. (11) is square and invertible.

Consider a one-dimensional three-degree-of-freedom spring–mass system, shown in Fig. 3, whose global mass $[M]$ and global stiffness $[K]$ matrices are, respectively,

$$[M] = \begin{bmatrix} m_1 & 0 & 0 \\ 0 & m_2 & 0 \\ 0 & 0 & m_3 \end{bmatrix}, \qquad [K] = \begin{bmatrix} (k_1 + k_2) & -k_2 & 0 \\ -k_2 & (k_2 + k_3) & -k_3 \\ 0 & -k_3 & k_3 \end{bmatrix} \tag{46}$$

and whose element stiffness submatrices ($L = 3$) are

$$\left[K_1^e\right] = \begin{bmatrix} k_1 & 0 & 0 \\ 0 & 0 & 0 \\ 0 & 0 & 0 \end{bmatrix}, \qquad \left[K_2^e\right] = \begin{bmatrix} k_2 & -k_2 & 0 \\ -k_2 & k_2 & 0 \\ 0 & 0 & 0 \end{bmatrix}$$

$$\left[K_3^e\right] = \begin{bmatrix} 0 & 0 & 0 \\ 0 & k_3 & -k_3 \\ 0 & -k_3 & k_3 \end{bmatrix} \tag{47}$$

The arbitrarily chosen healthy SDPs are shown in Table 2. A simulated multiple damage scenario is examined with exact damage distributions shown in Table 2 with stiffness reductions of 1% for spring 1, 15% for spring 2, and 6.25% for spring 3. The SDP values

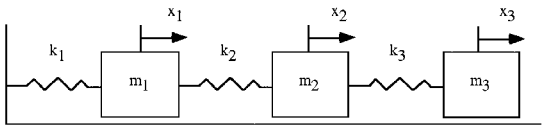


**Fig. 3 One-dimensional three-degree-of-freedom spring–mass system.**

**Table 2 Healthy and exact damaged distributions for the spring–mass system**

| Type | Structural parameter | Distribution | Correlation coefficient matrix |
|---|---|---|---|
| Healthy system | $k_1$ | $N(10, 0.1)$ | $[\rho_k] = \begin{bmatrix} 1 & 0.25 & 0.75 \\ 0.25 & 1 & 0.5 \\ 0.75 & 0.5 & 1 \end{bmatrix}$ |
| | $k_2$ | $N(3, 0.03)$ | |
| | $k_3$ | $N(8, 0.08)$ | |
| | $m_1$ | $N(6, 0.06)$ | $[\rho_m] = \begin{bmatrix} 1 & 0.9 & 0.5 \\ 0.9 & 1 & 0.75 \\ 0.5 & 0.75 & 1 \end{bmatrix}$ |
| | $m_2$ | $N(4, 0.04)$ | |
| | $m_3$ | $N(4, 0.04)$ | |
| Exact damage | $\tilde{k}_1$ | $N(9.9, 0.1485)$ | $[\tilde{\rho}_k] = \begin{bmatrix} 1 & 0.45 & 0.65 \\ 0.45 & 1 & 0.45 \\ 0.65 & 0.4 & 1 \end{bmatrix}$ |
| | $\tilde{k}_2$ | $N(2.55, 0.0510)$ | |
| | $\tilde{k}_3$ | $N(7.5, 0.075)$ | |

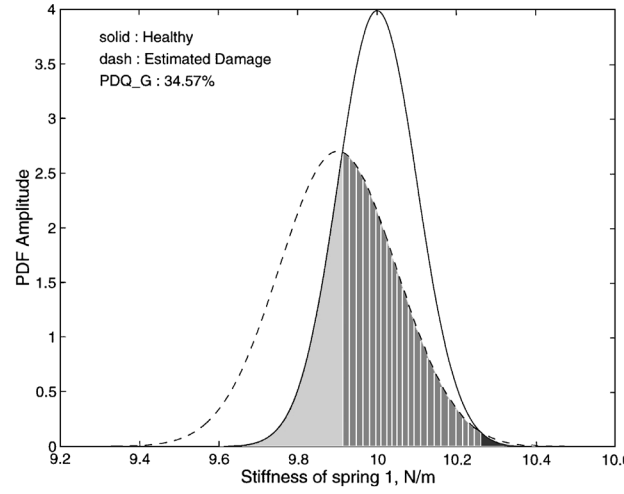


**Fig. 4 Healthy and estimated damage stiffness PDF comparison using the graphical approach, for spring 1.**

consist of $\{k_1, k_2, k_3, m_1, m_2, m_3, \tilde{k}_1, \tilde{k}_2, \tilde{k}_3, m_1, m_2, m_3\}$; therefore, $P = 12$ (six healthy SDPs and six damaged SDPs) and $N = 3$ because all three modes were used.

The SRF correlation coefficient matrix was calculated using 100,000 Monte Carlo simulations and is given in Table 3 together with the mean SRFs obtained by the application of Eq. (14). During the simulation, damaged modal parameters were randomly generated by conducting eigenanalyses on randomly generated mass and damaged stiffness matrices. Not surprisingly, using the exact mean values of the eigenvalues and eigenvectors in Eq. (14) clearly found the exact mean SRFs for each spring. The Monte Carlo simulations also agreed well with Eq. (14) results.

The statistical properties of the estimated damaged stiffnesses are listed in Table 4. Comparisons of Tables 2 and 4 indicate that the proposed method accurately estimated the exact damage distributions with a maximum standard deviation error of less than 1.6%. The correlation coefficient matrix for the damaged stiffnesses was also accurately estimated with a maximum error of less than 3.9%. If 50,000 Monte Carlo simulations were performed rather than 100,000, the maximum damaged stiffness standard deviation and correlation coefficient errors would increase to 2.77 and 6.27%, respectively. Graphically comparing the healthy and estimated damaged stiffness PDF curves yields the PDQs, which are listed in Table 4 and graphically shown in Fig. 4 for spring 1 and in Fig. 5a for spring 2 and Fig. 5b for spring 3. Results indicate that springs 2 and 3 were definitely damaged with 100 and 99.88% PDQ-Gs, respectively. The PDQ-Gs for springs 2 and 3 indicate that the healthy and damaged distributions essentially do not share any common stiffness values; hence, damage is definitely present. Spring 1, on the other hand, had a 34.57% PDQ-G, which indicates that some form of damage occurred, but not at the level of springs 2 and 3.

In contrast, Table 5 lists the PDQ-S for $\pm 1\sigma$, $\pm 2\sigma$, and $\pm 3\sigma$ healthy intervals, and the shaded area in Fig. 6 shows the PHQ-S for

**Table 3 SRF distributions from the Monte Carlo simulation for the spring–mass system**

| SRF | Mean value equation (14) | Monte Carlo simulation | Correlation coefficient matrix |
|---|---|---|---|
| $\alpha_1$ | −0.01 | $N(-0.0098, 0.0237)$ | $[\rho_{SRF}] = \begin{bmatrix} 1 & 0.351 & 0.699 \\ 0.351 & 1 & 0.580 \\ 0.699 & 0.580 & 1 \end{bmatrix}$ |
| $\alpha_2$ | −0.15 | $N(-0.1499, 0.0232)$ | |
| $\alpha_3$ | −0.0625 | $N(-0.0623, 0.0181)$ | |

**Table 4 Estimated damaged distributions for the spring–mass system**

| SDP | Distribution | Correlation coefficient matrix | PDQ-G, % |
|---|---|---|---|
| $\tilde{k}_1$ | $N(9.9, 0.1476)$ | $[\tilde{\rho}_k] = \begin{bmatrix} 1 & 0.433 & 0.641 \\ 0.433 & 1 & 0.396 \\ 0.641 & 0.396 & 1 \end{bmatrix}$ | 34.57 |
| $\tilde{k}_2$ | $N(2.55, 0.0517)$ | | 100 |
| $\tilde{k}_3$ | $N(7.5, 0.0739)$ | | 99.88 |

**Table 5 PDQ-S comparisons of ± 1$\sigma$, ± 2$\sigma$, and ± 3$\sigma$ healthy intervals for the spring–mass system**

| | PDQ-S% | | |
|---|---|---|---|
| $\pm n\sigma$ Interval | $\tilde{k}_1$ | $\tilde{k}_2$ | $\tilde{k}_3$ |
| 1 | 58.77 | 100.00 | 100.00 |
| 2 | 27.01 | 100.00 | 100.00 |
| 3 | 9.11 | 100.00 | 99.98 |

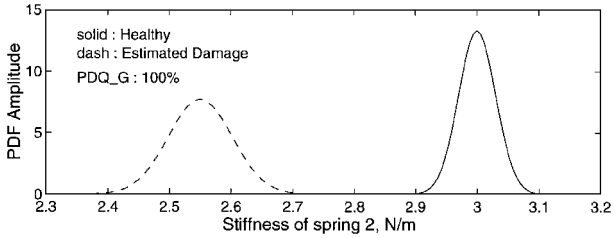


**a) Spring 2**

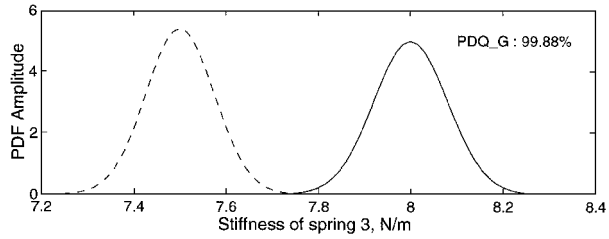


**b) Spring 3**

**Fig. 5 Healthy and estimated damage stiffness PDF comparisons using the graphical approach.**

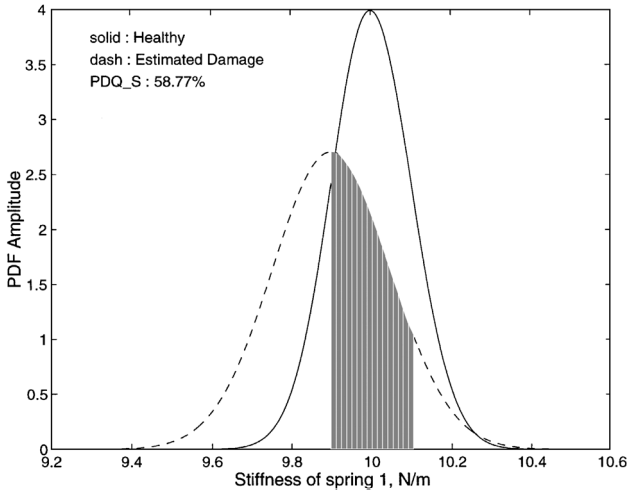


**Fig. 6 Healthy and estimated damage stiffness PDF comparison for spring 1 using a ± 1$\sigma$ healthy interval in the statistical approach.**

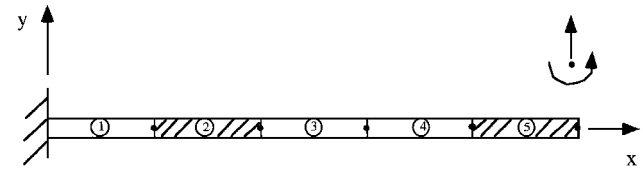


**Fig. 7 Euler–Bernoulli cantilever beam discretized by a uniform mesh of five beam elements.**

spring 1 using a $\pm 1\sigma$ interval. Springs 2 and 3 have essentially 100% PDQ-S irrespective of the size of the healthy interval; therefore, damage is clearly indicated. Spring 1, on the other hand, has a substantial range: 58.77% ($\pm 1\sigma$), 27.01% ($\pm 2\sigma$), and 9.11% ($\pm 3\sigma$). Depending on the interval size chosen, i.e., values for $n$, spring 1 may or may not be considered damaged. One can determine, based on the SRF statistics, PDQ-G/PDQ-S, and experience, whether or not to consider spring 1 as a damaged spring. Overall, the method properly detected, located, and estimated the simulated damage.

Next, the complexity of the analyzed system is increased by considering an Euler–Bernoulli cantilever aluminum beam that has been discretized using a uniform mesh of five beam elements, shown in Fig. 7 with two degrees of freedom per node, i.e., a transverse translation and a rotation. The normal random quantities are the mass $m$ and flexural rigidity $EI$ per beam element. The consistent mass matrix approach was used in the FE model. A simulated multiple damage scenario is examined with elements two and five having flexural rigidity reductions of 2.5 and 5.0%, respectively (damage shown in Fig. 7 by the cross-hatched regions). The healthy and exact damage beam element distributions are shown in Table 6. All beam elements are of rectangular cross section with widths of 0.0381 m (1.5 in.) and thicknesses of 0.00635 m (0.25 in.), and each of the five elements are of length 0.1524 m (6 in.). The mean modulus of elasticity, mean density, cross-sectional area, and inertia were assumed to be 70 GPa, 2757.09 kg/m$^3$, 2.4191$E$-04 m$^2$, and 8.1279$E$-10 m$^4$, respectively. For this example, $N = 5$ (because the first five modes were used), $L = 5$ (because there are five elements), and $P = 20$ (10 healthy and 10 damaged SDPs).

The results from a 60,000 Monte Carlo simulation are listed in Table 7, and Table 8 provides the statistical properties of the estimated damaged flexural rigidities. Comparison of Tables 6 and 8 indicate that the proposed method accurately estimated the exact damage stiffness distributions with a maximum standard deviation error of less than 1.7%. The correlation coefficient matrix for the damaged flexural rigidities was also accurately estimated with a maximum error of less than 2.9%. If 30,000 Monte Carlo simulations were performed rather than 60,000, the maximum damaged stiffness standard deviation error would increase to 3.23% and the maximum correlation coefficient error would decrease slightly to 2.51%. Graphically comparing the healthy and estimated damaged stiffness PDF curves yields the probability damage quotients listed in Table 8. Beam elements 1, 3, and 4 had PDQ-Gs of less than 1%, indicating essentially no probability of damage. Beam elements 2 and 5, on the other hand, had PDQ-Gs of 91.31 and 96.05%, respectively, indicating a high degree of potential probable damage.

Table 9 lists the PDQs for each beam element using the statistical approach. The graphical and statistical PDF comparisons for elements 1–5 are similar to Figs. 4–6 and, therefore, are not shown. Elements 1, 3, and 4 have essentially identical PDQ-S values at the same interval size. The PDQ-S values for element 2 fluctuate significantly depending on the interval size from 99.89% at a $\pm 1\sigma$ interval to 15.39% at a $\pm 3\sigma$ interval. Element 5 is relatively insensitive to the interval size with a PDQ-S approximately greater than 92%. At

**Table 6 Healthy and exact damaged distributions for the cantilever beam elements**

| Type | SDP | Distribution | Correlation coefficient matrix |
|---|---|---|---|
| Healthy system | $EI_1$ | $N(56.8955, 0.5690)$ | $[\rho_{EI}] = \begin{bmatrix} 1 & 0.89 & 0.90 & 0.85 & 0.90 \\ 0.89 & 1 & 0.95 & 0.90 & 0.84 \\ 0.90 & 0.95 & 1 & 0.80 & 0.80 \\ 0.85 & 0.90 & 0.80 & 1 & 0.96 \\ 0.90 & 0.84 & 0.80 & 0.96 & 1 \end{bmatrix}$ |
| | $EI_2$ | $N(56.8955, 0.5690)$ | |
| | $EI_3$ | $N(56.8955, 0.5690)$ | |
| | $EI_4$ | $N(56.8955, 0.5690)$ | |
| | $EI_5$ | $N(56.8955, 0.5690)$ | |
| | $m_1$ | $N(0.1016, 0.001016)$ | $[\rho_m] = \begin{bmatrix} 1 & 0.90 & 0.90 & 0.80 & 0.90 \\ 0.90 & 1 & 0.80 & 0.85 & 0.93 \\ 0.90 & 0.80 & 1 & 0.90 & 0.75 \\ 0.80 & 0.85 & 0.90 & 1 & 0.80 \\ 0.90 & 0.93 & 0.75 & 0.80 & 1 \end{bmatrix}$ |
| | $m_2$ | $N(0.1016, 0.001016)$ | |
| | $m_3$ | $N(0.1016, 0.001016)$ | |
| | $m_4$ | $N(0.1016, 0.001016)$ | |
| | $m_5$ | $N(0.1016, 0.001016)$ | |
| Exact damage | $\tilde{EI}_1$ | $N(56.8955, 0.5690)$ | $[\tilde{\rho}_{EI}] = \begin{bmatrix} 1 & 0.90 & 0.95 & 0.85 & 0.90 \\ 0.90 & 1 & 0.85 & 0.75 & 0.70 \\ 0.95 & 0.85 & 1 & 0.85 & 0.85 \\ 0.85 & 0.75 & 0.85 & 1 & 0.79 \\ 0.90 & 0.70 & 0.85 & 0.79 & 1 \end{bmatrix}$ |
| | $\tilde{EI}_2$ | $N(55.4731, 0.2774)$ | |
| | $\tilde{EI}_3$ | $N(56.8955, 0.5690)$ | |
| | $\tilde{EI}_4$ | $N(56.8955, 0.5690)$ | |
| | $\tilde{EI}_5$ | $N(54.0508, 0.8108)$ | |

**Table 7 SRF distributions from the Monte Carlo simulation for all beam elements**

| SRF | Mean value equation (14) | Monte Carlo simulation | Correlation coefficient matrix |
|---|---|---|---|
| $\alpha_1$ | 0.00 | $N(0.0001, 0.0199)$ | $[\rho] = \begin{bmatrix} 1 & 0.858 & 0.865 & 0.889 & 0.891 \\ 0.858 & 1 & 0.878 & 0.854 & 0.743 \\ 0.865 & 0.878 & 1 & 0.835 & 0.857 \\ 0.889 & 0.854 & 0.835 & 1 & 0.867 \\ 0.891 & 0.743 & 0.857 & 0.867 & 1 \end{bmatrix}$ |
| $\alpha_2$ | −0.025 | $N(-0.0248, 0.0174)$ | |
| $\alpha_3$ | 0.00 | $N(0.0002, 0.0200)$ | |
| $\alpha_4$ | 0.00 | $N(0.0002, 0.0200)$ | |
| $\alpha_5$ | −0.05 | $N(-0.0499, 0.0218)$ | |

**Table 8 Estimated damaged distributions for all beam elements**

| SDP | Distribution | Correlation coefficient matrix | PDQ-G, % |
|---|---|---|---|
| $\tilde{EI}_1$ | $N(56.8955, 0.5770)$ | $[\rho_{\tilde{EI}}] = \begin{bmatrix} 1 & 0.908 & 0.951 & 0.853 & 0.902 \\ 0.908 & 1 & 0.867 & 0.764 & 0.720 \\ 0.951 & 0.867 & 1 & 0.857 & 0.852 \\ 0.853 & 0.764 & 0.857 & 1 & 0.799 \\ 0.902 & 0.720 & 0.852 & 0.799 & 1 \end{bmatrix}$ | 0.68 |
| $\tilde{EI}_2$ | $N(55.4731, 0.2791)$ | | 91.31 |
| $\tilde{EI}_3$ | $N(56.8955, 0.5781)$ | | 0.77 |
| $\tilde{EI}_4$ | $N(56.8955, 0.5756)$ | | 0.56 |
| $\tilde{EI}_5$ | $N(54.0508, 0.8183)$ | | 96.05 |

**Table 9 PDQ-S comparisons of ± 1$\sigma$, ± 2$\sigma$, and ± 3$\sigma$ healthy intervals for the cantilever beam**

| | PDQ-S% | | | | |
|---|---|---|---|---|---|
| $\pm n\sigma$ Interval | $\tilde{EI}_1$ | $\tilde{EI}_2$ | $\tilde{EI}_3$ | $\tilde{EI}_4$ | $\tilde{EI}_5$ |
| 1 | 32.41 | 99.89 | 32.50 | 32.29 | 99.73 |
| 2 | 4.86 | 84.59 | 4.90 | 4.80 | 98.15 |
| 3 | 0.31 | 15.39 | 0.31 | 0.30 | 91.78 |

the $\pm 2\sigma$ interval, the PDQ-S clearly indicates that elements 2 and 5 are damaged. On the other hand, at the $\pm 3\sigma$ interval, element 5 is clearly damaged, but element 2 may or may not be considered damaged, depending on whether one considers 15.39% a high damage indicator. Overall, as in the earlier example, the method correctly detected, located, and estimated the simulated damage.

## Conclusions

A method has been presented to improve the robustness characteristics of current damage detection methodologies. Measured statistical changes in natural frequencies and mode shapes along with a correlated analytical stochastic FE model are used to assess the integrity of a structure. Structural damage was characterized by a change in stiffness only, and the mass was assumed unchanged. The approach accounts for structural variability, e.g., in natural frequencies and mode shapes, due to experimental errors in the test procedure. The structural parameters of the system were modeled as correlated normal random variables. This permitted the determination of probability damage quotients per structural element. These quotients indicate a confidence level on the existence of damage and provide a means of adding robustness to the damage identification problem. Simulated data were used in the analysis to determine multiple damage of the order of 1–6% (light damage) and 15% (severe damage). Coincidentally, because the beam example had very light damage levels, this may be considered as an application of the theory to the model update/refinement problem. Overall, the method was successful in identifying the probabilistic existence, location, and extent of simulated structural damage in a one-dimensional three-degree-of-freedom spring–mass system and an Euler–Bernoulli cantilever aluminum beam.

## References

[1] Kashangaki, T. A.-L., "On-Orbit Damage Detection and Health Monitoring of Large Space Trusses—Status and Critical Issues," *Proceedings of the AIAA/ASME/ASCE/AHS/ASC 32nd Structures, Structural Dynamics, and Materials Conference*, AIAA, Washington, DC, 1991, pp. 2947–2958 (AIAA Paper 91-1181, April 1991).

[2] Doebling, S. W., Farrar, C. R., Prime, M. B., and Shevitz, D. W., "Damage Identification and Health Monitoring of Structural and Mechanical Systems from Changes in Their Vibration Characteristics: A Literature Review," Los Alamos National Lab., LA-13070-MS, UC-900, Los Alamos, NM, May 1996.

[3] Vandiver, J. K., "Detection of Structural Failure on Fixed Platforms by Measurement of Dynamic Response," *Journal of Petroleum Technology*, March 1977, pp. 305–310.

[4] Cawley, P., and Adams, R. D., "The Location of Defects in Structures

from Measurements of Natural Frequencies," *Journal of Strain Analysis*, Vol. 14, No. 2, 1979, pp. 49–57.

[5]Hassiotis, S., and Jeong, G. D., "Assessment of Structural Damage from Natural Frequency Measurements," *Computers and Structures*, Vol. 49, No. 4, 1993, pp. 679–691.

[6]Yuen, M. M. F., "A Numerical Study of the Eigenparameters of a Damaged Cantilever," *Journal of Sound and Vibration*, Vol. 103, 1985, pp. 301–310.

[7]Wolff, T., and Richardson, M., "Fault Detection in Structures from Changes in Their Modal Parameters," *Proceedings of the 7th International Modal Analysis Conference* (Las Vegas, NV), Union College, Schenectady, NY, 1989, pp. 87–94.

[8]Pandey, A. K., Biswas, M., and Samman, M. M., "Damage Detection from Changes in Curvature Mode Shapes," *Journal of Sound and Vibration*, Vol. 145, No. 2, 1991, pp. 321–332.

[9]Chen, J. C., and Garba, J. A., "On-Orbit Damage Assessment for Large Space Structures," *AIAA Journal*, Vol. 26, No. 9, 1988, pp. 1119–1126.

[10]Kashangaki, T. A.-L., Smith, S. W., and Lim, T. W., "Underlying Modal Data Issues for Detecting Damage in Truss Structures," *Proceedings of the AIAA/ASME/ASCE/AHS/ASC 33rd Structures, Structural Dynamics, and Materials Conference*, AIAA, Washington, DC, 1992, pp. 1437–1446 (AIAA Paper 92-2264, April 1992).

[11]Collins, J. D., and Thomson, W. T., "The Eigenvalue Problem for Structural Systems with Statistical Properties," *AIAA Journal*, Vol. 7, No. 4, 1969, pp. 642–648.

[12]Hart, G. C., and Collins, J. D.,"The Treatment of Randomness in Finite Element Modeling" (Los Angeles, CA), Vol. 79, Society of Automotive Engineers, 1970, pp. 2509–2520 (SAE Paper 700842, Oct. 1970).

[13]Collins, J. D., Hart, G. C., and Kennedy, B.,"Statistical Analysis of the Modal Properties of Large Structural Systems" (Los Angeles, CA), Society of Automotive Engineers, 1971, pp. 1–10 (SAE Paper 710785, Sept. 1971).

[14]Hasselman, T. K., and Hart, G. C., "Modal Analysis of Random Structural Systems," *Journal of the Engineering Mechanics Division, Proceedings of the American Society of Civil Engineers*, Vol. 98, No. EM3, 1972, pp. 561–579.

[15]Collins, J. D., Hart, G. C., Hasselman, T. K., and Kennedy, B., "Statistical Identification of Structures," *AIAA Journal*, Vol. 12, No. 2, 1974, pp. 185–190.

[16]Ricles, J. M., and Kosmatka, J. B., "Damage Detection in Elastic Structures Using Vibratory Residual Forces and Weighted Sensitivity," *AIAA Journal*, Vol. 30, No. 9, 1992, pp. 2310–2316.

[17]Tavares, R., Kosmatka, J. B., Ricles, J. M., and Wicks, A., "Using Experimental Modal Data to Detect Damage in a Space Truss," *Proceedings of the AIAA/ASME/ASCE/AHS/ASC 34th Structures, Structural Dynamics, and Materials Conference*, AIAA, Washington, DC, 1993, pp. 1556–1564 (AIAA Paper 93-1486, April 1993).

[18]White, C. W., and Maytum, B. D., "Eigensolution Sensitivity to Parametric Model Perturbations," *Shock and Vibration Bulletin*, No. 46, Pt. 5, Aug. 1976, pp. 123–133.

[19]Lim, T. W., "A Submatrix Approach to Stiffness Matrix Correction Using Modal Test Data," *AIAA Journal*, Vol. 28, No. 6, 1990, pp. 1123–1130.

[20]Lim, T. W., "Structural Damage Detection Using Modal Test Data," *AIAA Journal*, Vol. 29, No. 12, 1991, pp. 2271–2274.

[21]Kleiber, M., and Hien, T. D., *The Stochastic Finite Element Method: Basic Perturbation Technique and Computer Implementation*, Wiley, 1992, pp. 1–100.

[22]Fox, R. L., and Kapoor, M. P., "Rates of Change of Eigenvalues and Eigenvectors," *AIAA Journal*, Vol. 6, No. 12, 1968, pp. 2426–2429.

G. A. Kardomateas
*Associate Editor*